

3DTCR: A Physics-Based Generative Framework for Vortex-Following 3D Reconstruction to Improve Tropical Cyclone Intensity Forecasting

Jun Liu¹, Xiaohui Zhong¹, Kai Zheng¹, Jiarui Li¹, Yifei Li¹, Tao Zhou², Wenxu Qian¹, Shun Dai³, Ruian Tie¹, Yangyang Zhao^{1,3} and Hao Li^{1,3*}

¹Artificial Intelligence Innovation and Incubation Institute, Fudan University, Shanghai, 200433, China.

²Department of Atmospheric and Oceanic Sciences, Institute of Atmospheric Sciences, Fudan University, Shanghai, 200438, China.

³Shanghai Academy of Artificial Intelligence for Science, Shanghai, 200232, China.

*Corresponding author(s). E-mail(s): lihao_lh@fudan.edu.cn;

Contributing authors: junliu23@m.fudan.edu.cn;

x7zhong@gmail.com; kaizheng.work@gmail.com;

jrli24@m.fudan.edu.cn; yfli23@m.fudan.edu.cn;

tzhou22@m.fudan.edu.cn; wxqian23@m.fudan.edu.cn;

sdai@sai.ais.cn; ratye23@m.fudan.edu.cn; yyzhao@fudan.edu.cn;

Abstract

Tropical cyclone (TC) intensity forecasting remains challenging as current numerical and AI-based weather models fail to satisfactorily represent extreme TC structure and intensity. Although intensity time-series forecasting has achieved significant advances, it outputs intensity sequences rather than the three-dimensional inner-core fine-scale structure and physical mechanisms governing TC evolution. High-resolution numerical simulations can capture these features but remain computationally expensive and inefficient for large-scale operational applications. Here we present 3DTCR, a physics-based generative framework combining physical constraints with generative AI efficiency for 3D

TC structure reconstruction. Trained on a six-year, 3-km-resolution moving-domain WRF dataset, 3DTCR enables region-adaptive vortex-following reconstruction using conditional Flow Matching(CFM), optimized via latent domain adaptation and two-stage transfer learning. The framework mitigates limitations imposed by low-resolution targets and over-smoothed forecasts, improving the representation of TC inner-core structure and intensity while maintaining track stability. Results demonstrate that 3DTCR outperforms the ECMWF high-resolution forecasting system (ECMWF-HRES) in TC intensity prediction at nearly all lead times up to 5 days and reduces the RMSE of maximum WS10M by 36.5% relative to its FuXi inputs. These findings highlight 3DTCR as a physics-based generative framework that efficiently resolves fine-scale structures at lower computational cost, which may offer a promising avenue for improving TC intensity forecasting.

Keywords: Tropical cyclone, Intensity forecasting, Vortex-following reconstruction, Physics-based, Conditional Flow Matching

1 Introduction

Accurate forecasting of tropical cyclone (TC) intensity and its three-dimensional (3D) dynamic evolution remains a critical yet incompletely resolved challenge in global meteorology [1](see Supplementary Fig. S1). The intensifying impacts of climate change are driving more frequent and destructive TCs, making precise intensity prediction essential for disaster mitigation and public safety [2–11]. Despite recent advances in AI weather prediction (AIWP) [12–16] and statistical sequence extrapolation, which have achieved remarkable success in predicting tracks [14–16] and numerical intensity values [17, 18], a one-dimensional intensity sequence remains insufficient to capture the complex dynamical structure of tropical cyclones. [19]

In operational practice, while a predicted intensity sequence is highly valuable, it is often insufficient for a comprehensive diagnosis [20]. When evaluating TC intensification, particularly rapid intensification (RI) [4, 20, 21], forecasters are increasingly seeking insights that extend beyond mere numerical metrics, aspiring to examine the actual internal structure [22, 23]. This is driven by the understanding that a grasp of the underlying physical processes and dynamic mechanisms is crucial for a complete assessment [4, 24]. Only by accurately depicting these complex inner-core structures can forecasters confidently determine a TC’s true intensity and reliably anticipate its subsequent evolution [25, 26]. However, current capabilities often fall short of this operational expectation. In characterizing 3D structures, both traditional numerical models and emerging AI foundation models continue to suffer from systematic underestimation [27–29]. This structural deficiency makes it exceedingly difficult to accurately quantify a TC’s true destructive power, maximum potential intensity (MPI), and broader impact range [26, 30–32]. Fundamentally, this shared

limitation stems from a resolution bottleneck: coarse-resolution global models (e.g., 25 km) simply cannot explicitly resolve fine-scale kinematic and thermodynamic processes [28], ultimately failing to capture the extreme intensity peaks and fine-scale structural features of severe TCs [26, 33].

TC intensity forecasting critically depends on high-resolution 3D data to resolve these inner-core structures [26, 34, 35]. However, obtaining such data remains challenging in practice. Actual 3D observations (e.g., aircraft dropsondes, satellite remote sensing, and ground-based radars) yield authentic measurements but are plagued by spatiotemporal discontinuity, multi-source heterogeneity, and prohibitive acquisition costs. [17, 36, 37]. Furthermore, access to these high-resolution dataset are frequently constrained by confidentiality and security protocols, precluding their use in large-scale model training [38]. Conversely, while reanalysis data (e.g., ERA5) offer spatiotemporal continuity, their inherently coarse resolution severely exacerbates the systematic underestimation of extreme inner-core gradients [28, 29]. This deficiency is further compounded in AI models by the “double penalty” problem [39], which forces overly smoothed predictions to minimize spatial phase errors. Relying exclusively on real-time, high-resolution numerical weather prediction (NWP) to bypass this resolution bottleneck is equally impractical; despite its physical realism, the exponentially scaling computational overhead limits its deployment in real-time operations and large-scale applications [40, 41]. Consequently, constructing a high-resolution historical simulation dataset offline emerges as a pragmatic, cost-effective strategy to provide the critical fine-scale supervision signals required for model training.

To bridge this resolution gap, AI-based statistical downscaling methods have been widely explored and have achieved notable progress in reconstructing high-resolution TC structures [42–48]. However, in complex scenarios, existing methods still face two closely related challenges. First, most models rely on fixed computational domains and limited variables [49]. Because TCs evolve and migrate across vast oceans, fixed-grid designs can introduce substantial irrelevant background noise, reducing spatial flexibility and limiting the ability to adaptively track moving storm cores. In addition, few-variable settings are often insufficient to represent the full 3D TC structure and may weaken the coupled dynamical constraints across multi-level meteorological fields that govern intensity change [50, 51]. Second, these limitations further complicate the modeling of the long-tail distribution of extreme intensity peaks. Deterministic models optimized with general loss functions (e.g., L_1 or L_2) mathematically tend to predict conditional means, leading to over-smoothing, suppressed high-frequency gradients, and underestimation of critical extremes, especially for rare extreme intensification events such as rapid intensification from category 4 to 5 [52]. Probabilistic generative models have recently been introduced to address this issue. Diffusion models [45–47, 53–55] can recover fine-scale details, but their iterative sampling remains computationally expensive. For practical TC applications, balancing detailed structure generation, sampling efficiency, and the incorporation of TC-relevant physical

constraints remains challenging. Moreover, error propagation across denoising steps may still limit the representation of compact core structures, sharp gradients, and extreme-intensity peaks, leaving room for further improvement in physically consistent high-resolution generation [56, 57]. More recently, continuous normalizing flows, particularly flow matching, have shown clear advantages in trajectory learning and sampling efficiency [58–62]. Yet how to integrate this efficient generative framework with the 3D dynamical characteristics of TCs, so as to preserve physical structural consistency while accurately capturing extreme-intensity tails, remains an open question [11].

To address these fundamental bottlenecks, we present 3DTCR, a physics-based generative framework to drastically reduce the computational overhead of high-resolution TC downscaling while preserving the physical constraints of dynamical models. The framework is developed upon a purpose-built 7-year, 3-km resolution dataset, generated via independent $10^\circ \times 10^\circ$ dynamic moving region WRF simulations centered on historical TC tracks. From the full suite of 93 output variables, we distill 21 multi-level meteorological variables to capture the vertical thermodynamic and kinematic structure of the TC inner core. Built upon this dataset, 3DTCR employs a region-adaptive, vortex-following architecture [63], integrating a dynamic TC tracking algorithm with conditional flow matching (CFM), focusing its generative capacity on reconstructing the core vortex structure. This targeted design circumvents the prohibitive computational costs of traditional large-domain or moving-nest NWP simulations, effectively unifying the physical generalizability of dynamical models with the sampling efficiency of generative AI. To further mitigate the cumulative spatial pattern shift and error accumulation inherent in long-lead global AI forecasts (e.g., FuXi), we devise a two-stage, time-aware latent domain alignment strategy. Evaluations show that 3DTCR reasonably captures radial wind gradients and fine-scale three-dimensional structural features, achieving orders-of-magnitude computational acceleration while surpassing the operational ECMWF-HRES model in extreme intensity prediction across nearly all lead times up to 5 days.

2 Results

2.1 Constructing physically high-resolution ground truth

Unlike track prediction, which is largely governed by large-scale environmental flows, intensity forecasting depends strongly on the detailed structure of the TC inner core. For global reanalysis data commonly used in large model training (e.g., ERA5), capturing these detailed features is a major challenge. Due to limited spatial resolution, these models often fail to resolve the sharp wind speed gradients and extreme values within the TC inner core. Furthermore, many key physical processes occur at subgrid scales, preventing accurate representation of extreme TC intensities.

To address this, we constructed the 3DTC vortex-region high-resolution dataset (WRF-3km) via dynamical downscaling (See Section S1.4 of the Supplementary Information for detailed numerical simulation procedures and parameter settings.). Visual comparisons (see Supplementary Fig. S3) show that the 3-km simulation better resolves the fine-scale structure of the inner core, whereas these features appear blurred in coarse-resolution data. Resolving such details is essential for accurately representing extreme intensity.

To ensure the data quality, we conducted a comprehensive validation, as supported by the distribution analysis in Fig. 1. In terms of overall performance, the 3DTC vortex-region high-resolution dataset (WRF-3km) significantly reduces errors compared to other datasets. Specifically, compared to FuXi, our dataset reduces the overall Bias by 72.2% and RMSE by 47.9%. Similarly, it achieves overall improvements of 69.2% in Bias and 42.9% in RMSE over ERA5. Notably, even when compared to the industry-leading ECMWF-HRES system, our dataset still shows clear advantages, reducing the overall Bias by 49.3% and RMSE by 25.2%. These results confirm that the 3DTC dataset is closer to actual observations, providing the more reliable and physically consistent supervision signals needed for effective model training.

2.2 Overall tropical cyclone intensity forecast performance

Building upon the training dataset validated in the previous section, achieving efficient dynamic reconstruction of the adaptive TC vortex structure and ensuring its applicability to practical operational scenarios are the key problems addressed in this study. To validate the effectiveness of the proposed scheme, we conducted a comprehensive statistical evaluation. Fig. 1 visualizes the correlation between predicted and observed (IBTrACS) maximum wind speeds. Evidently, standard baselines (FuXi and ERA5) exhibit a distinct limitation where the underestimation becomes increasingly pronounced as the TC intensity strengthens. Distinguished from conventional approaches that rely on TC intensity sequence extrapolation, our method is dedicated to the reconstruction of the fine-scale TC structure. This capability enables a physical tracing of the potential physical dynamic processes behind TC intensification, aligning with the critical operational requirement to diagnose the structural mechanisms governing intensity evolution. Fig. 1 also presents the performance of other methods involved in the optimization process (detailed analysis of these ablation methods is discussed in subsequent subsections).

As expected, this fine-scale structural reconstruction effectively overcomes the intensity bottlenecks stemming from the over-smoothing effect inherent in AI-based large models as forecast lead time increases, as well as the inherent underestimation in reanalysis data. As illustrated in Fig. 1(i), compared to the baselines (FuXi, ERA5, and ECMWF-HRES), the proposed scheme designed for operational scenarios demonstrates a distribution pattern that is significantly closer to the observations (IBTrACS), effectively narrowing the gap seen in these baselines.

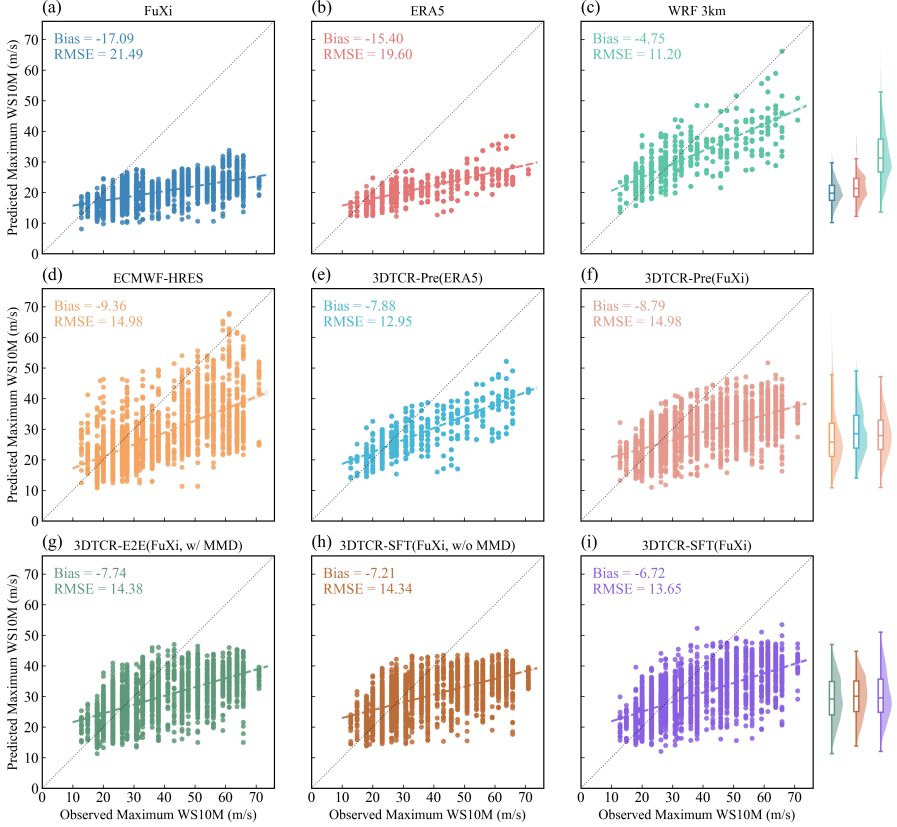


Fig. 1: Scatter plot comparison of maximum 10-m wind speed (WS10M) predictions across different methods. Panels (a–i) display the correlation between predicted and observed (IBTrACS) values for 2,242 test samples pooled across all forecast lead times from the 2024 Northwest Pacific dataset. Solid lines denote the global linear regression fit with 95% confidence intervals, contrasted against the ideal 1:1 reference (dashed lines). The right-most column illustrates the marginal distributions via box plots overlaid on kernel density estimates (KDEs), while the inset values represent the global Mean Bias and RMSE metrics.

We further evaluated the detailed TC intensity error characteristics at various lead times throughout the 5-day forecast period. Referring to the error evolution visualized in Fig. 2a, the error distribution characteristics in Fig. 2b, and the detailed statistical metrics summarized in table 1, we analyzed the evolution of prediction errors from 6 to 120 hours. The results reveal distinct error growth patterns: while the errors of AI-based large models (e.g., FuXi) rise steeply and quickly exceed 20 m/s after the 24-hour mark, the proposed

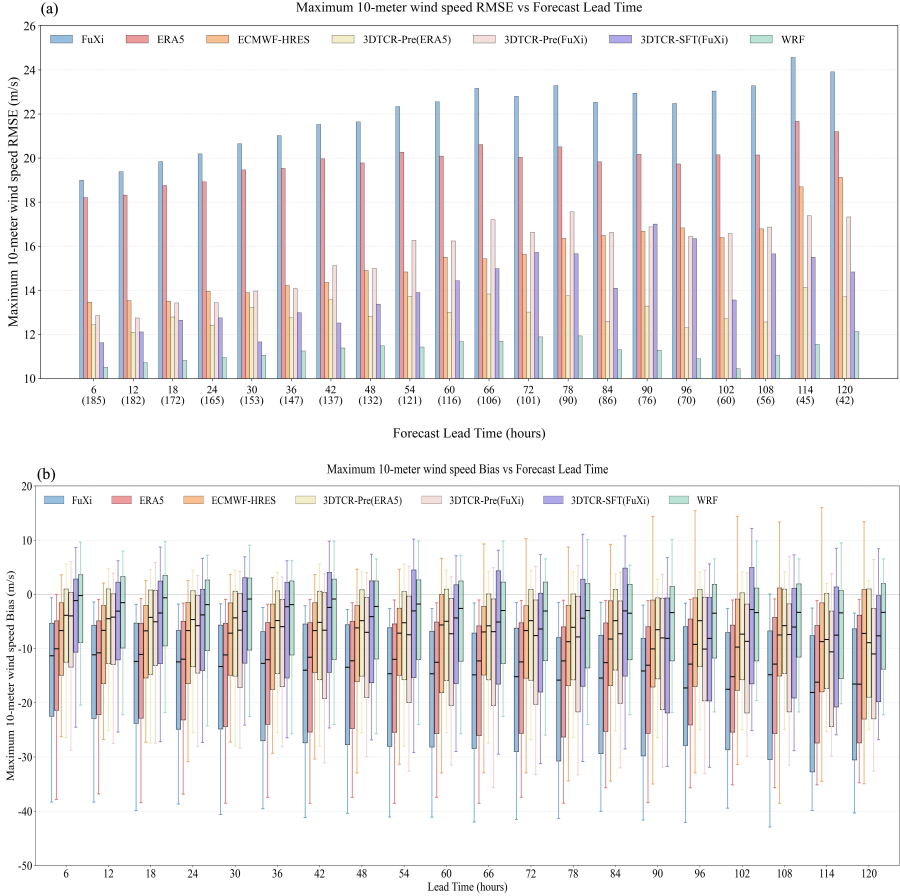


Fig. 2: Evaluation of maximum 10-meter wind speed forecasts across lead times. (a) RMSE versus forecast lead time, with numbers in parentheses denoting sample sizes. (b) Box-and-whisker plots of forecast bias (model minus observation), where boxes represent the interquartile range (IQR) and horizontal lines indicate the median. Both panels compare standard baselines—FuXi (blue), ERA5 (red), ECMWF-HRES (orange), and WRF (green)—against the proposed 3DTCR framework: pre-trained models using ERA5 (beige) or FuXi (pink) inputs, and the final SFT model (purple).

scheme maintains a relatively stable performance. Specifically, in the long-term forecast window from 24 to 120 hours, 3DTCR keeps the RMSE within a low range of 13–14 m/s, demonstrating superior stability compared to the baselines.

Quantitatively, as detailed in [table 1](#), the proposed scheme demonstrates robust improvements over all baselines. Specifically, it reduces the RMSE by

36.5% and TC intensity Bias by 60.7% compared to the FuXi input, effectively compensating for the coarse resolution. Moreover, it achieves a 30.4% RMSE improvement over ERA5, surpassing the TC intensity estimation performance of standard reanalysis data. Remarkably, our scheme outperforms the industry-leading ECMWF-HRES operational system across almost all lead times, achieving a relative RMSE improvement of 8.9% and a Bias reduction of 28.2%. This confirms that the proposed scheme offers robust TC intensity improvement throughout the forecast period.

Table 1: RMSE Performance of 10-meter Maximum Wind Speed Prediction (Lower is Better ↓)

Method	24h	48h	72h	96h	120h
Baselines					
FuXi	20.19	21.64	22.80	22.94	23.91
ERA5	18.92	19.77	20.04	20.17	21.20
ECMWF-HRES	13.96	14.90	15.63	16.68	19.12
Ours					
3DTCR-E2E(FuXi, w/ MMD)	13.55	15.06	16.67	16.56	15.32
3DTCR-Pre(ERA5)	12.42	12.82	13.01	13.28	13.71
3DTCR-Pre(FuXi)	13.43	14.99	16.64	16.44	17.33
3DTCR-SFT(FuXi, w/o MMD)	12.99	14.19	16.32	17.05	15.38
3DTCR-SFT(FuXi, w/MMD)	12.75	13.37	15.72	16.34	14.83
Target					
WRF	10.95	11.47	11.89	11.28	12.13

2.3 Reconstruction of fine-scale 3D structures of TCs

To further investigate the fine-scale reconstruction capabilities of 3DTCR, we conduct a detailed analysis of Super Typhoon KONG-REY (2024) as a representative extreme case. In late October 2024, KONG-REY rapidly intensified into a Category 5-equivalent storm, reaching a maximum sustained wind speed of 72 m/s at its peak intensity, along with a minimum central pressure of 925 hPa. It made landfall in Taitung, Taiwan, causing direct economic losses exceeding \$167 million. Here, we utilize this case to verify 3DTCR’s performance in characterizing fine-scale structures.

2.3.1 Three-Dimensional Structural Characteristics

Horizontal Circulation Structure. The accurate representation of the three-dimensional vortex structure is fundamental to diagnosing TC intensity and evolution. We begin by analyzing the horizontal distribution of key physical quantities. Fig. 3 presents the surface-level reconstruction results for Typhoon KONG-REY at an 18-hour lead time. Initialized at 12:00 UTC on October 29, 2024, the forecast targets the validation time of 06:00 UTC on October 30, 2024. The figure compares five key variables: 2-meter temperature (T2M), 10-meter wind components (U10M, V10M), mean sea level pressure (MSL), and 10-meter wind speed (WS10M). As shown in the first row, the input from FuXi tends to be smooth, exhibiting a blurred pattern of the storm. Notably, based on this smoothed guidance, the 3DTCR output (second row) better reconstructs the TC vortex structure. It enhances the intensity based on the input conditions, effectively capturing finer physical structures and providing a refined representation of the inner core dynamics.

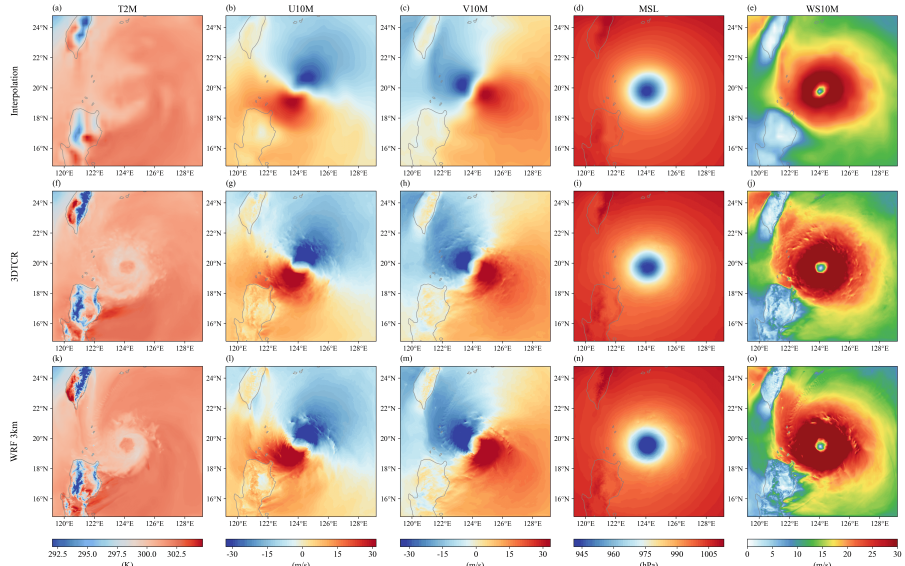


Fig. 3: Typhoon KONG-REY multi-variable field reconstruction at 18-h forecast lead time. Reconstruction comparison of the TC vortex structure through 2-meter temperature (T2M, K), 10-meter u/v wind components (U10M, V10M, m/s), mean sea level pressure (MSL, hPa), and 10-meter wind speed (WS10M, m/s), initialized at 12 UTC October 29, 2024. Rows from top to bottom: Interpolation (FuXi), 3DTCR reconstruction, and WRF 3km simulation (ground truth).

To verify the generalization capability and robustness of 3DTCR across different initialization times and forecast horizons, we provide additional comparisons in the Supplementary Material. Supplementary Fig. S6 illustrates the reconstruction of Typhoon KONG-REY at a 96-hour lead time. Furthermore, we validate the model on other severe typhoons, including Typhoon YAGI and Typhoon YINXING (see Supplementary Figs. S7, S8, and S9), covering a wide range of lead times from 18 to 108 hours. Similar to the KONG-REY case, 3DTCR demonstrates stable performance in these scenarios. As expected, the model accurately captures the sharp radial gradients distinguishing the weak-wind eye from the eyewall, effectively resolving the radius of maximum wind (RMW) and the complex asymmetric spiral structures of the vortex.

Vertical Wind Structure. Complementing the horizontal structure analysis, we first examine the internal structure of the tropical cyclone from a vertical perspective. Supplementary Fig. S10 illustrates the zonal and meridional vertical cross-sections of wind speed for Typhoon KONG-REY, capturing the weak-wind eye surrounded by deep, high-wind speed columns. The azimuthally averaged wind components (see Supplementary Fig. S11) further reveal the dynamic mechanisms maintaining the vortex. By filtering out asymmetric perturbations, the tangential wind profile displays a robust rotating column, while the radial wind profile uncovers a coherent secondary circulation (low-level inflow and upper-level outflow). This structure aligns with the physics of mature tropical cyclones, suggesting that the reconstructed field reasonably maintains the transport of moisture and angular momentum.

Multi-level Circulation Patterns. In terms of spatial distribution, the 3DTCR model reconstructs the horizontal circulation patterns across different tropospheric levels (500 hPa, 850 hPa, and Surface), as shown in Supplementary Figs. S12, S13, S14, and S15. The concentric geopotential height fields and wind distributions reflect the structural integrity of the vortex. The physical realism of these structures is further corroborated by overlaying the reconstructed 10-m surface wind field onto a satellite cloud image (see Supplementary Fig. S16). The alignment between the spiraling wind vectors and the observed cloud bands—particularly the inflow arms—supports the plausibility of the results, indicating that the model-generated surface circulation is reasonable relative to the observed convective organization.

Dynamic Evolution. Beyond the static analysis, Supplementary Fig. S17 tracks the temporal evolution of the system. The time-series analysis of wind speed and geopotential height effectively captures the translation of the vortex center and reflects morphological changes, such as the contraction of the wind field during intensification. This demonstrates the model’s capability to capture the dynamic lifecycle of the tropical cyclone.

Generalization Verification. A similar analysis was conducted for Typhoon YAGI to further validate the robustness of the proposed method (see Supplementary Figs. S22, S20, S21, S23, S24, S25, S26, and S27 in the Supplementary Information). The reconstruction of this independent case exhibits vertical wind speed distributions and circulation patterns comparable to those

of Typhoon KONG-REY. These consistent results across different typhoon events suggest that the model has good generalization capability.

2.3.2 Multi-scale Spectra and Harmonic Analysis

Multi-scale Energy Analysis. While the previous sections demonstrated the model’s capability in reconstructing the macroscopic 3D morphology, it is equally critical to evaluate the fidelity of the wind field from a statistical and energetic perspective. In atmospheric flows, kinetic energy is predominantly concentrated in large-scale synoptic patterns (low wavenumbers), while it naturally decays at smaller scales (high wavenumbers). However, numerical smoothing often leads to an accelerated attenuation of energy in the high-frequency band, which hinders the accurate depiction of fine-scale structures. Energy spectra thus serve as a diagnostic tool to verify whether the downscaling process maintains a realistic energy distribution across scales. Complementarily, PDFs are used to evaluate the model’s ability to represent the full range of variability, particularly the tail distribution corresponding to extreme wind events. We take Typhoon KONG-REY as a representative example to conduct this comparative analysis, as shown in Fig. 4. The PDF analysis (Column 2) indicates that the coarse-resolution input tends to underestimate the probability of high wind speeds, exhibiting a narrower distribution. The 3DTCR output, however, shows a broader distribution that aligns more closely with the WRF benchmark, suggesting an improved representation of extreme intensities. In the spectral domain (Columns 3 and 4), all models show consistent energy levels at low wavenumbers, capturing the dominant circulation patterns. At high wavenumbers, the input fields exhibit a rapid drop-off in energy, reflecting the inherent smoothness of the global forecast. In contrast, the 3DTCR spectrum exhibits a slower decay rate, comparable to that of the WRF simulation. This suggests that the model helps alleviate the energy deficiency at small scales, potentially recovering some of the high-frequency variability lost in the coarser input. A similar multi-scale energy analysis was also conducted for Typhoon YAGI (see Supplementary Fig. S28), which produced similar findings. In particular, 3DTCR better reproduces the broader wind speed distribution and the slower high-wavenumber spectral decay than the coarse-resolution input, further supporting the robustness and generalization capability of the proposed method.

Harmonic Structure Assessment. To further evaluate structural complexity, we employ azimuthal Fourier decomposition (see Supplementary Figs. S18 and S19). The symmetric component (wavenumber 0) dictates the mean vortex flow, whereas higher-order harmonics (wavenumbers ≥ 1) capture highly nonlinear asymmetric perturbations. Recovering these complex high-frequency modes is inherently challenging, making their accurate reconstruction a rigorous metric for structural realism. Results indicate that the interpolation baseline is heavily dominated by the symmetric mode and lacks meaningful asymmetry. In contrast, 3DTCR successfully recovers the spectral signatures of harmonics up to wavenumber 20. The reconstructed amplitudes

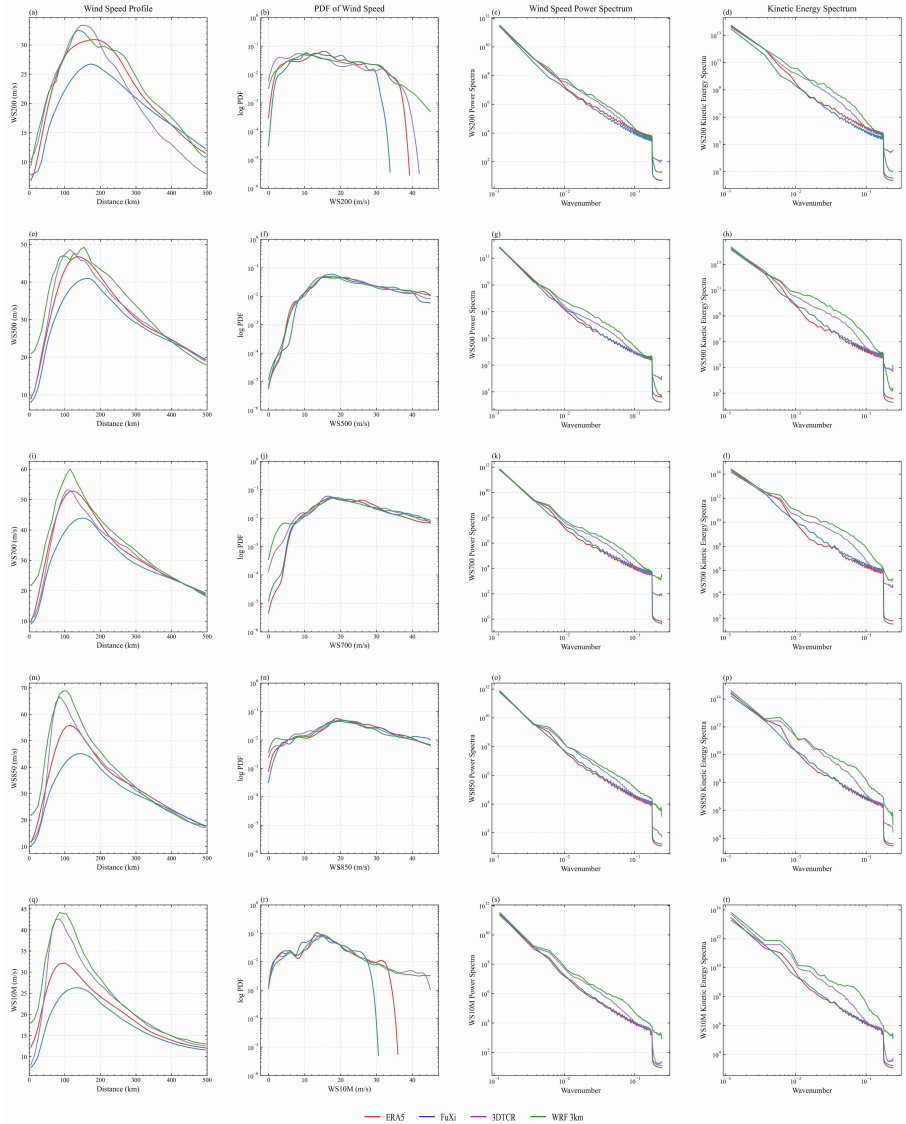


Fig. 4: Multi-level wind speed profiles and spectral analysis for Typhoon KONG-REY. Evolution of wind speed characteristics across different atmospheric levels: 200 hPa (first row), 500 hPa (second row), 700 hPa (third row), 850 hPa (fourth row), and 10-meter height (fifth row). Each row shows: wind speed profiles along distance (first column), probability density functions of wind speed (second column), wind speed power spectra (third column), and kinetic energy spectra (fourth column). Results are compared among ERA5 reanalysis (red), FuXi forecast (blue), 3DTCR model (purple), and WRF 3km simulation (green). Power and kinetic energy spectra are displayed in log-log scale, revealing the multi-scale characteristics and energy cascade of the typhoon circulation.

align closely with the ground truth, demonstrating the model’s capacity to infer plausible asymmetric features, including convective spiral bands, which remain under-resolved in the coarse input data. A similar harmonic analysis was also conducted for Typhoon YAGI (see Supplementary Figs. S29 and S30). Consistent with the results for Typhoon KONG-REY, 3DTCR more faithfully captures both the dominant symmetric structure and the higher-order asymmetric harmonics than the interpolation baseline. These results further support the robustness and generalization capability of the proposed method.

2.4 Ablation Study: Effectiveness of Two-Stage Training and Latent Space Domain Adaptation

In operational scenarios, there is a significant distribution gap between forecast fields and ground-truth reanalysis data. This gap appears as “pattern shifts” that increase with lead time, causing systematic spatial displacement and intensity bias. Direct reconstruction from such inputs is challenging: simple regression models fail to capture high-frequency textures, while generative models without explicit guidance struggle to balance bias correction and detail generation, often leading to a smoothing effect that loses extreme values. To accurately evaluate performance in these difficult cases, especially for extreme weather events, we use the Critical Success Index (CSI). Unlike standard error metrics, CSI is sensitive to how well the model captures extreme features in the long-tail distribution.

Based on this metric, the ablation results in Fig. 5 clearly demonstrate the impact of different optimization strategies on extreme event detection. First, we verify the importance of the domain adaptation mechanism. Comparing the variant without latent space domain adaptation (3DTCR-SFT w/o MMD, green bars) to the full model (purple bars) reveals that lacking this adaptation leads to significantly lower performance across all wind speed thresholds. This quantitative drop is visually corroborated in Fig. 5. Thanks to latent space domain adaptation, the model maintains structural integrity and accurately recovers extreme intensities (e.g., the typhoon eye wall) even with large spatial shifts at long lead times, rather than simply smoothing them out. This confirms that domain adaptation is essential to bridge the substantial distribution gap between the input and the target.

Furthermore, to investigate the training strategy, we compared the one-stage end-to-end model (3DTCR-E2E, yellow bars) with the two-stage model using the same domain adaptation (purple bars). Notably, although the E2E model employs multi-task optimization, its performance drops significantly when facing challenging extreme events (e.g., WS10M > 32.7 m/s, Fig. 5). This suggests that balancing distribution alignment and detail generation simultaneously in a single stage is highly difficult. In contrast, our proposed two-stage strategy demonstrates a clear advantage. By decoupling the task into adapting the base distribution in the first stage and focusing on detail recovery in the second, the model achieves consistently high CSI scores, particularly for

Model Performance Comparison: Critical Success Index (CSI)

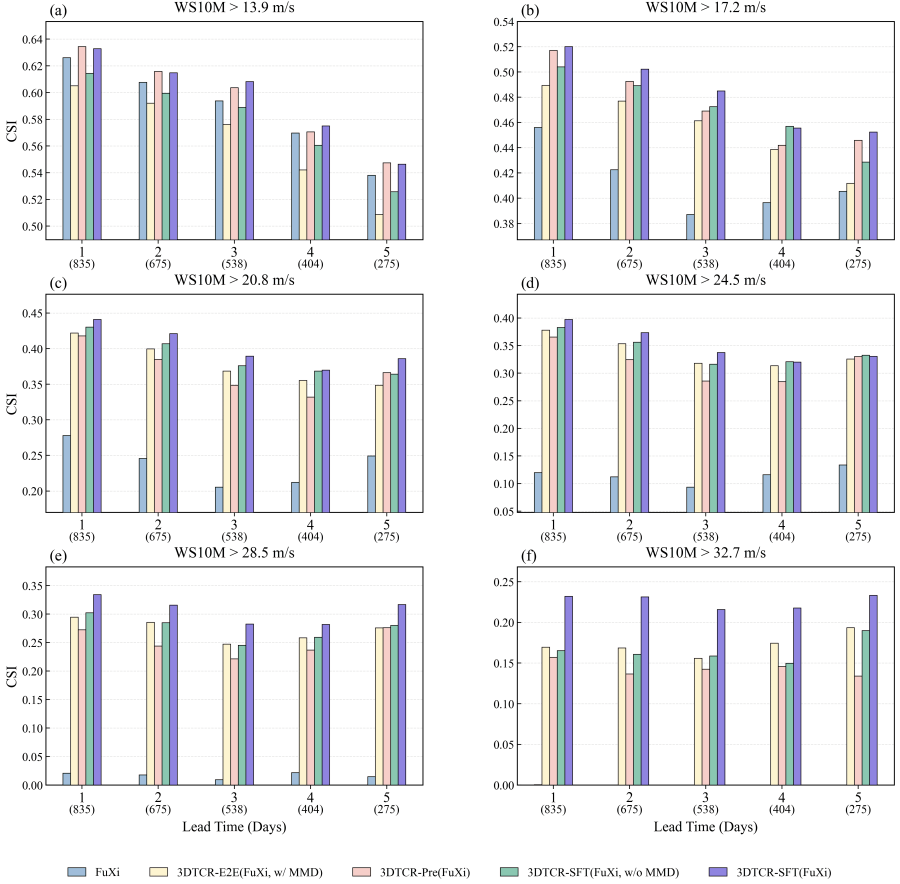


Fig. 5: Ablation analysis of 3DTCR using different training strategies. Comparison of Critical Success Index (CSI) scores for maximum 10-m wind speed (WS10M) at lead times of 1 to 5 days, as an indicator of extreme intensity forecasting skill. Panels (a–f) correspond to six increasing intensity thresholds ranging from 13.9 to 32.7 m/s. The bar groups illustrate the FuXi baseline alongside 3DTCR variants trained using different optimization strategies (Pre-training, SFT, and E2E) and multi-task loss settings (with or without MMD).

extremes. These results prove that, under identical loss constraints, a step-by-step strategy reconstructs extreme structures more effectively, significantly improving the representation of long-tail features.

2.5 Computational Efficiency and Adaptive Region Reconstruction Strategy

A significant challenge in high-resolution modeling is the computational cost associated with large-scale simulations. While generating 3 km resolution data over the entire Western North Pacific is theoretically possible, the computational cost increases drastically with the domain size, making such an approach impractical for real-time applications. To address this issue, we adopt an adaptive region reconstruction strategy. Instead of reconstructing the entire basin, our method specifically targets the TC vortex structure within a localized $10^\circ \times 10^\circ$ window. This strategy focuses computational resources on the most critical weather system rather than the large background area. The efficiency improvement from this approach is substantial. As shown in Supplementary Table S2, a standard WRF simulation at 3 km resolution requires over 400 hours on a 32-core CPU cluster due to the large grid size. In contrast, by limiting the domain to the dynamic vortex and using deep learning acceleration, 3DTCR completes the fine-scale structural reconstruction within minutes on a single GPU. This method effectively overcomes the computational bottleneck of traditional simulations while maintaining the necessary structural details.

3 Discussion

Accurate TC intensity forecasting requires not only precise numerical prediction but also faithful representation of the underlying three-dimensional physical structures and dynamical processes. Although sequence-based approaches using historical tracks have improved numerical intensity prediction, reliance on a single one-dimensional intensity value remains insufficient for operational diagnosis, particularly over the vast ocean, where capturing the evolving three-dimensional vortex structure is critical. To bridge this gap, we propose 3DTCR, a generative dynamical 3D vortex-following reconstruction framework. By explicitly repairing and reconstructing the fine-scale inner-core structures of TCs at an aligned spatial resolution, 3DTCR successfully recovers sharp radial gradients and extreme wind speeds. As shown in our overall statistical evaluation (see Table 1), 3DTCR robustly outperforms operational systems such as ECMWF-HRES across almost all lead times, providing reliable structural support for revealing TC intensity evolution.

The ability of 3DTCR to break through existing bottlenecks lies fundamentally in its deep integration of AI generative efficiency with the physical laws of high-resolution numerical models, alongside a clever decoupling of intensity and phase learning. First, from a physical reconstruction perspective, traditional numerical weather prediction (NWP) relies on highly complex and computationally expensive “vortex-following moving nests” to track vortices. In contrast, the training dataset for 3DTCR consists of moving regions centered on the TC, prompting the model to learn intrinsic vortex features independent of absolute spatial coordinates. Combined with an efficient generative architecture and a tracking algorithm, the model achieves dynamic moving

reconstruction with exceptionally high computational efficiency (as detailed in Section 2.5) while successfully preserving the physically plausible fine-scale features derived from rigorous WRF simulations. Second, from an optimization perspective, global AI models inevitably suffer from cumulative errors and pattern shifts at long lead times. To mitigate this, we designed a two-stage training paradigm coupled with latent domain adaptation. The pre-training stage focuses on learning the intensity mapping, while the fine-tuning stage introduces a lead-time-aware Maximum Mean Discrepancy (MMD) mechanism. This precisely aligns the features of the biased operational forecasts (FuXi) with the reanalysis domain, effectively decoupling the learning of intensity and phase. As demonstrated by the ablation study (Fig. 5), this mechanism successfully mitigates the suboptimal extreme wind speed reconstruction caused by spatial pattern shifts.

Although 3DTCR demonstrates significant advantages in physical structure reconstruction and computational efficiency, this study still has certain limitations regarding ground truth approximation, extreme error handling, and engineering deployment. First, the WRF-simulated dataset is inherently an approximation of the true atmospheric state. Different physical parameterization schemes significantly affect the simulated intensity, and whether the scheme adopted here is optimal requires further verification. Consequently, as indicated by the scatter analysis (see Fig. 1), a gap remains between the reconstructed results and the actual IBTrACS observations. Second, while the two-stage training and domain adaptation mitigate the smoothing issues caused by cumulative errors, they do not completely eliminate them, leaving room to improve model robustness under extreme forecast deviations. Third, although 3DTCR inference is highly efficient, the current pipeline, which consists of global AI-based meteorological forecasting, regional cropping, and TC vortex reconstruction, remains somewhat cumbersome for practical operational deployment. Exploring a unified “end-to-end” architecture, where a single model directly outputs improved TC intensity forecasts, is a crucial future direction for simplifying engineering deployment.

In conclusion, this study demonstrates that extending pure statistical sequence extrapolation to physically plausible 3D structural reconstruction is a highly promising path for advancing data-driven TC intensity forecasting. By deeply integrating the efficient generative capabilities of AI with the physical constraints of numerical models, this region-adaptive, physics-informed framework proves that AI can successfully resolve the critical fine-scale features driving TC evolution without imposing a prohibitive computational burden. As AI meteorological foundation models continue to evolve, such lightweight and physically plausible reconstruction solutions will provide a vital reference paradigm for future operational TC forecasting and disaster mitigation.

4 Materials and Methods

4.1 Data

We employed the Weather Research and Forecasting (WRF) model [64] to simulate high-resolution tropical cyclone (TC) events in the western North Pacific. These simulations were driven by ERA5 reanalysis data [65] at 0.25° resolution as initial and boundary conditions (see Supplementary Information Section S1.2). Detailed WRF configurations are provided in see Supplementary Information Section S1.4.

Distinct from traditional computationally intensive multi-layer nesting schemes, we adopted a dynamic single-domain strategy. Specifically, we performed independent moving simulations for each sample by centering a standalone $10^\circ \times 10^\circ$ domain strictly on the coordinates provided by the International Best Track Archive for Climate Stewardship (IBTrACS). To focus on significant convective systems, we restricted our simulations to TC events classified as Tropical Storm intensity or higher, defined by maximum sustained wind speeds exceeding 17.2 m/s in the IBTrACS records. This approach efficiently resolves fine-scale convective structures at 3-km resolution. The simulation generated 1,903 samples, each containing 93 meteorological variables across multiple pressure levels. We regridded the outputs to 0.027° (370×370 grid points) to create the spatial ground truth, using IBTrACS as the benchmark for intensity and track validation. To support model fine-tuning and benchmarking, we also included operational forecast data from the FuXi model (see Supplementary Information Section S1.3) and the ECMWF High-Resolution (HRES) system .

To balance memory constraints with computational efficiency, we select key atmospheric variables strongly correlated with TC intensity for model training (see Supplementary Information Section S1.5). Specifically, we choose geopotential height (Z), temperature (T), and horizontal wind components (U, V) at four critical pressure levels spanning the lower to upper troposphere (850 hPa, 700 hPa, 500 hPa, and 200 hPa), together with five surface variables: 2-meter temperature (T2M), mean sea level pressure (MSL), 10-meter wind speed (WS10M), and 10-meter wind components (U10M, V10M). This configuration captures the three-dimensional structure of TCs and yields 21 variables in total. Simultaneously, we implemented a two-stage training framework. The pre-training stage uses only ERA5 reanalysis to learn fundamental physical mappings. Subsequently, the fine-tuning stage introduces a multi-task objective optimization to realize latent space domain adaptation (details in Supplementary Information Section S2.4). To support this, we integrated both ERA5 reanalysis and operational FuXi forecast data in this phase, applying a MMD loss to mitigate pattern deviations. The training dataset spans from 2018 to 2023, with the 2024 used as the test set.

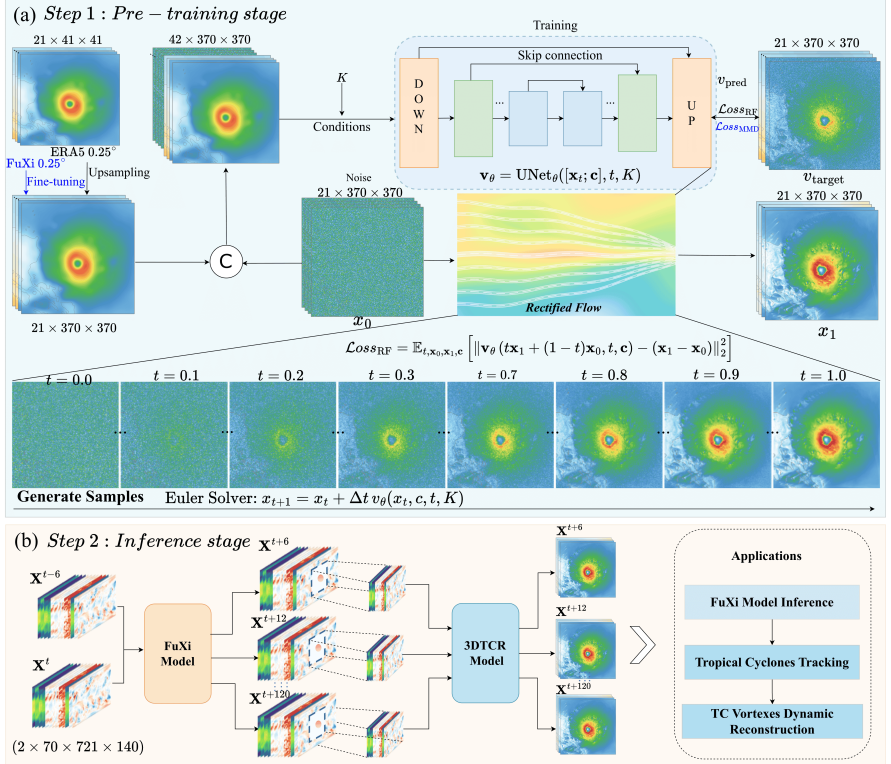


Fig. 6: Schematic diagram of the overall framework of the 3DTCR model. (a) **Training stage:** The model is first pre-trained on ERA5 reanalysis data via Rectified Flow to learn the velocity field, followed by fine-tuning (indicated by blue arrows) with both ERA5 and operational FuXi forecast data using an MMD loss to align latent feature distributions. (b) **Inference stage:** FuXi forecasts are dynamically tracked and cropped to TC-centered regions, serving as inputs to the 3DTCR model to reconstruct high-resolution TC vortex structures at each time step, enabling improved TC forecasting.

4.2 3DTCR model architecture

To circumvent the prohibitive computational costs of traditional dynamical downscaling while effectively resolving the fine-scale structures of tropical cyclones (TCs), we propose the 3DTCR framework. This architecture is designed as a physics-informed conditional generative model, trained on high-resolution (3 km) numerical simulation data derived from dynamical models. Consequently, the model implicitly learns to generate atmospheric states that adhere to the structural characteristics of TCs, ensuring kinematic continuity and thermodynamic balance. The framework is founded on a probabilistic

generative paradigm utilizing Conditional Flow Matching (for details on Rectified Flow, see Section S2.2 in the Supplementary Information.) to establish a non-linear mapping from coarse-resolution global forecasts to high-resolution mesoscale fields (see Fig. 6). The network input is formed by concatenating randomly sampled Gaussian noise x_0 ($21 \times 370 \times 370$) with resolution-aligned coarse-grained background conditions c , yielding a combined input of dimension $42 \times 370 \times 370$. Simultaneously, the forecast lead time K also serves as a global condition governing the diffusion process. Structurally, the velocity field estimator is instantiated as a U-Net backbone, featuring a symmetric encoder-decoder design with three levels of downsampling and upsampling to capture multi-scale features. The model is optimized by minimizing the Rectified Flow loss L_{RF} to learn a velocity field v_θ , which defines the transport trajectory evolving from noise to the target atmospheric state.

The framework implementation progresses through a coarse-to-fine optimization strategy. Initially, a pre-training phase utilizes exclusively ERA5 reanalysis data spatially aligned with the target labels to learn fundamental physical mappings. Subsequently, loading this pre-trained model as the backbone, the fine-tuning phase introduces a multi-task objective to achieve latent space domain adaptation (see Supplementary Information Section S2.4). In this stage, we integrate operational FuXi forecast data alongside reanalysis data and apply a MMD loss. This critical step mitigates the systematic pattern shifts and distribution discrepancies that accumulate with increasing forecast lead times, ensuring the model adapts to the specific characteristics of forecast data.

Finally, the inference stage leverages the model’s location-agnostic capability through a Region-Adaptive Reconstruction Strategy. Since the model is optimized on moving windows centered on the TC vortex, it learns intrinsic local dynamics rather than location-specific background features, effectively decoupling the vortex structure from absolute geospatial coordinates. Exploiting this property, the inference process integrates a lightweight tracking algorithm (see Supplementary Information Section S2.1) with the predictive FuXi weather model (initialized from two historical atmospheric states). In this operational workflow, the algorithm dynamically locates the moving TC center, allowing the framework to extract and reconstruct a localized $10^\circ \times 10^\circ$ domain (covering a spatial extent exceeding 1000 km). This enables the efficient reconstruction of the target region. This object-centric approach is functionally analogous to the “vortex-following moving nest” technique in classical Numerical Weather Prediction (NWP). However, unlike traditional methods which typically necessitate computationally intensive stepwise integration, our approach achieves orders-of-magnitude higher efficiency. By concentrating computational resources on resolving critical inner-core dynamics, this strategy effectively captures fine-scale TC structural features, thereby improving TC intensity forecasting.

4.3 Time-Aware Latent Domain Adaptation via MMD to Mitigate Extreme Underestimation

The accumulation of forecast errors remains a major challenge in AI-based weather forecasting. As lead times increase, upstream foundation models inevitably produce forecasts with severe spatial phase shifts. When downstream downscaling models utilize these heavily biased forecasts as inputs, the massive mismatch between the degraded input and the ideal high-resolution target triggers a severe “double penalty” effect [39]. To minimize this penalty under high uncertainty, models inherently exhibit a strong regression to the mean, yielding over-smoothed outputs. This statistical compromise leads to a systematic underestimation of extremes, completely failing to characterize peak intensities and fine-scale vortex structures.

To better represent these extremes even when the input deviates significantly, we propose a time-aware latent domain adaptation strategy. Since our model is pre-trained on reanalysis data (ERA5) to learn the mapping to high-resolution fields, the ERA5 distribution serves as an ideal target domain rich in extreme features. During the fine-tuning stage, we employ a dual-input mechanism to correct the forecast features. Specifically, recognizing that forecast errors exacerbate over time, we incorporate the forecast lead time (step) as a conditioning variable to render the model time-aware. Concurrently, we use MMD to pull the biased forecast features toward the ERA5 reference distribution within the latent space. This combined approach helps alleviate the smoothing tendency caused by the double penalty, enabling the model to better preserve extreme intensities and clear vortex structures even at longer lead times. (Detailed mathematical derivations of the MMD loss are provided in Supplementary Information Section S2.5.2.)

4.4 3DTCR model architecture and training

As illustrated in Fig. 6, 3DTCR adopts a physics-informed generative architecture based on Rectified Flow, where the velocity field estimator is parameterized by a symmetric U-Net backbone. The model reconstructs high-resolution tropical cyclone structures by capturing both large-scale environmental flow and fine-scale inner-core dynamics through hierarchical encoder-decoder representations. Attention modules are incorporated into the deep latent layers to enhance long-range spatial dependency modeling, and a forecast lead-time conditioning mechanism is introduced to account for the distinct error characteristics associated with different lead times.

To mitigate the domain shift between reanalysis and forecast data, 3DTCR employs a coarse-to-fine two-stage transfer learning strategy. In the pre-training stage, the model is trained using ERA5 inputs and WRF targets to learn the fundamental physical downscaling mapping under a relatively stable reanalysis distribution. In the supervised fine-tuning stage, ERA5 and FuXi forecast data are jointly used as inputs, and the pre-trained model is optimized through a multi-objective learning scheme. Specifically, this stage combines a

reconstruction objective for WRF target recovery with an MMD-based latent-space domain alignment objective that regularizes the bottleneck features, thereby reducing the distribution discrepancy between ERA5 and FuXi in the latent-space domain while preserving the physically consistent structures learned during pre-training. By coupling transfer learning with latent-space domain adaptation, 3DTCR improves the reconstruction of localized extreme winds, particularly in the tropical cyclone inner-core region. Detailed formulations of the loss functions, network configuration, lead-time embedding, and optimization settings are provided in Supplementary Information Section S2.5.

4.5 Experimental Design and Ablation Framework

To evaluate our proposed training strategies, we designed an ablation study. All 3DTCR model variants use the same U-Net backbone and use WRF 3-km simulations as the high-resolution ground truth. Our ablation study examines two key aspects: the effectiveness of the two-stage training approach in reducing training difficulty, and the effectiveness of latent feature alignment. Specifically, to test the two-stage strategy, we compared it with a one-stage end-to-end variant (3DTCR-E2E) trained from scratch. Furthermore, to test the effect of the MMD loss, we evaluated a two-stage variant fine-tuned only with the MSE loss (3DTCR-SFT w/o MMD). This variant maps biased forecasts to the target without aligning the data distributions. Detailed information about the training strategies, configurations, and loss function combinations for all models can be found in Supplementary Table S4.

4.6 Evaluation metrics

We evaluate the 3DTCR model from both macro-sequence and micro-spatial perspectives using IBTrACS as the ground truth. At the sequence level, TC track errors are evaluated by the Mean Absolute Error (MAE) of storm-center positions, while WS10M intensity errors are measured by the Root Mean Square Error (RMSE) and Bias. To further assess the reconstruction of fine-scale extreme wind structures, we adopt the Critical Success Index (CSI) across multiple WS10M thresholds corresponding to different TC intensity stages. Detailed definitions of all metrics are provided in Supplementary Information Section S2.7.

Data availability

We downloaded a subset of the ERA5 dataset from the official website of Copernicus Climate Data (CDS) at <https://cds.climate.copernicus.eu/>. The TIGGE data set is available at <https://apps.ecmwf.int/datasets/data/tigge/levtype=sfc/type=cf/>. ECMWF HRES TC tracks were retrieved from the TIGGE archive in the form of downloadable XML files, which can be accessed via <https://confluence.ecmwf.int/display/TIGGE/Tools>. Additionally, we obtained the ground truth tracks of TC from the International

Best Track Archive for Climate Stewardship (IBTrACS) project, which is publicly available at <https://www.ncei.noaa.gov/products/international-best-track-archive>. The WRF model is available at https://www2.mmm.ucar.edu/wrf/users/download/get_source.html. TDR products are available at <https://www.aoml.noaa.gov/ftp/pub/hrd/data/radar/level3/>. Places2 data set is available via <http://places2.csail.mit.edu>. Himawari satellite data were obtained from the Japan Meteorological Agency (JMA), with general information available at <https://www.jma.go.jp/jma/jma-eng/satellite/>, and the data can be downloaded from the JAXA P-Tree system at <https://www.eorc.jaxa.jp/ptree/>.

Code availability

The 3DTCR related code used for evaluation in this study are publicly available and can be accessed from : <https://github.com/JunLiu88/3DTCR>.

Acknowledgements

We thank ECMWF for providing the ERA5 reanalysis dataset and HRES forecasts, and acknowledge the WeatherBench2 ensemble forecast data available through Google Cloud. We are grateful to NOAA National Centers for Environmental Information for maintaining the IBTrACS dataset. We express our sincere gratitude to Prof. Jie Feng from the Department of Atmospheric and Oceanic Sciences at Fudan University for his valuable guidance and insightful suggestions throughout this research. We also thank Shanghai Academy of Artificial Intelligence for Science (SAIS) for providing the internship opportunity, during which this work was primarily completed. The computations were performed using the Computing for the Future at Fudan (CFFF) platform.

Author Contributions

Jun Liu constructed, post-processed, and validated the dataset; designed the experimental and evaluation frameworks; trained and evaluated the model; and wrote the manuscript. Xiaohui Zhong contributed to project planning, reviewed the manuscript, and provided valuable guidance. Kai Zheng, Shun Dai, and Wenxu Qian conducted a subset of comparative experiments. Jiarui Li performed data visualization and contributed to manuscript preparation. Yifei Li contributed to a subset of the model evaluation. Tao Zhou conducted the TC mechanism analysis. Ruian Tie and Yangyang Zhao provided suggestions and guidance. Hao Li supervised the project, led the overall planning and management, and served as the corresponding author.

Funding

This research was supported by the National Natural Science Foundation of China (Grant No. 42505143) and the AI for Science Program, Shanghai Municipal Commission of Economy and Informatization (Grant No. 2025-GZL-RGZN-BTBX02017).

Ethics declarations

The authors declare no competing interests.

References

- [1] Emanuel, K.: 100 years of progress in tropical cyclone research. *Meteorological Monographs* **59**, 15–1 (2018)
- [2] Zhong, Q., Chan, J.C., Duan, W., Tu, S., Li, J., Gan, J., Ding, R.: Land-falling tropical cyclones accelerate due to land–sea thermal and roughness contrasts. *Nature Geoscience*, 1–6 (2026)
- [3] Rui, Z., Lin, L., Lu, H., Cheng, Y.F.: Climate research is global—risks and responsibilities should also be distributed. *Nature* **651**(8104), 274–274 (2026)
- [4] Kossin, J.P., Knapp, K.R., Olander, T.L., Velden, C.S.: Global increase in major tropical cyclone exceedance probability over the past four decades. *Proceedings of the National Academy of Sciences* **117**(22), 11975–11980 (2020)
- [5] Murakami, H., Delworth, T.L., Cooke, W.F., Zhao, M., Xiang, B., Hsu, P.-C.: Detected climatic change in global distribution of tropical cyclones. *Proceedings of the National Academy of Sciences* **117**(20), 10706–10714 (2020)
- [6] Emanuel, K.: Increasing destructiveness of tropical cyclones over the past 30 years. *Nature* **436**(7051), 686–688 (2005)
- [7] Mendelsohn, R., Emanuel, K., Chonabayashi, S., Bakkensen, L.: The impact of climate change on global tropical cyclone damage. *Nature climate change* **2**(3), 205–209 (2012)
- [8] Peduzzi, P., Chatenoux, B., Dao, H., De Bono, A., Herold, C., Kossin, J., Mouton, F., Nordbeck, O.: Global trends in tropical cyclone risk. *Nature climate change* **2**(4), 289–294 (2012)
- [9] Zhang, Q., Wu, L., Liu, Q.: Tropical cyclone damages in china 1983–2006. *Bulletin of the American Meteorological Society* **90**(4), 489–496 (2009)

- [10] Jewson, S.: The interpretation and implications of the knutson et al. 2020 projections of changes in the frequency and intensity of tropical cyclones under climate change. *Quarterly Journal of the Royal Meteorological Society* **148**(746), 2219–2242 (2022)
- [11] Kochkov, D., Yuval, J., Langmore, I., Norgaard, P., Smith, J., Mooers, G., Klöwer, M., Lottes, J., Rasp, S., Düben, P., *et al.*: Neural general circulation models for weather and climate. *Nature* **632**(8027), 1060–1066 (2024)
- [12] Shi, Y., Hu, R., Wu, N., Zhang, H., Liu, X., Zeng, Z., Zhu, J., Han, P., Luo, C., Zhang, H., *et al.*: Comparison of ai and nwp models in operational severe weather forecasting: A study on tropical cyclone predictions. *Journal of Geophysical Research: Machine Learning and Computation* **2**(2), 2024–000481 (2025)
- [13] Pathak, J., Subramanian, S., Harrington, P., Raja, S., Chattopadhyay, A., Mardani, M., Kurth, T., Hall, D., Li, Z., Azizzadenesheli, K., *et al.*: Fourcastnet: A global data-driven high-resolution weather model using adaptive fourier neural operators. *arXiv preprint arXiv:2202.11214* (2022)
- [14] Bi, K., Xie, L., Zhang, H., Chen, X., Gu, X., Tian, Q.: Accurate medium-range global weather forecasting with 3d neural networks. *Nature* **619**(7970), 533–538 (2023)
- [15] Chen, L., Zhong, X., Zhang, F., Cheng, Y., Xu, Y., Qi, Y., Li, H.: Fuxi: a cascade machine learning forecasting system for 15-day global weather forecast. *npj climate and atmospheric science* **6**(1), 190 (2023)
- [16] Lam, R., Sanchez-Gonzalez, A., Willson, M., Wirnsberger, P., Fortunato, M., Alet, F., Ravuri, S., Ewalds, T., Eaton-Rosen, Z., Hu, W., *et al.*: Learning skillful medium-range global weather forecasting. *Science* **382**(6677), 1416–1421 (2023)
- [17] Huang, C., Mu, P., Zhang, J., Chan, S., Zhang, S., Yan, H., Chen, S., Bai, C.: Benchmark dataset and deep learning method for global tropical cyclone forecasting. *Nature Communications* **16**(1), 5923 (2025)
- [18] Wang, X., Chen, K., Liu, L., Han, T., Li, B., Bai, L.: Global tropical cyclone intensity forecasting with multi-modal multi-scale causal autoregressive model. In: *ICASSP 2025-2025 IEEE International Conference on Acoustics, Speech and Signal Processing (ICASSP)*, pp. 1–5 (2025). IEEE
- [19] Chen, X., Luo, J.-J., Li, Q., Meng, F.: Meteorologically-informed adaptive conformal prediction for tropical cyclone intensity forecasting. *Journal of Geophysical Research: Machine Learning and Computation* **2**(4), 2025–000830 (2025)

- [20] Bhatia, K., Baker, A., Yang, W., Vecchi, G., Knutson, T., Murakami, H., Kossin, J., Hodges, K., Dixon, K., Bronselaer, B., *et al.*: A potential explanation for the global increase in tropical cyclone rapid intensification. *Nature communications* **13**(1), 6626 (2022)
- [21] Wang, C., Yang, N., Li, X.: Advancing forecasting capabilities: A contrastive learning model for forecasting tropical cyclone rapid intensification. *Proceedings of the National Academy of Sciences* **122**(4), 2415501122 (2025)
- [22] Li, Y., Tang, Y., Wang, S., Toumi, R., Song, X., Wang, Q.: Recent increases in tropical cyclone rapid intensification events in global offshore regions. *Nature Communications* **14**(1), 5167 (2023)
- [23] Knutson, T., Camargo, S.J., Chan, J.C., Emanuel, K., Ho, C.-H., Kossin, J., Mohapatra, M., Satoh, M., Sugi, M., Walsh, K., *et al.*: Tropical cyclones and climate change assessment: Part ii: Projected response to anthropogenic warming. *Bulletin of the American Meteorological Society* **101**(3), 303–322 (2020)
- [24] Chen, X., Rozoff, C.M., Rogers, R.F., Corbosiero, K.L., Tao, D., Gu, J.-F., Judt, F., Hendricks, E.A., Wang, Y., Bell, M.M., *et al.*: Research advances on internal processes affecting tropical cyclone intensity change from 2018–2022. *Tropical Cyclone Research and Review* **12**(1), 10–29 (2023)
- [25] Emanuel, K., Zhang, F.: The role of inner-core moisture in tropical cyclone predictability and practical forecast skill. *Journal of the Atmospheric Sciences* **74**(7), 2315–2324 (2017)
- [26] Roberts, M.J., Camp, J., Seddon, J., Vidale, P.L., Hodges, K., Vanniere, B., Mecking, J., Haarsma, R., Bellucci, A., Scoccimarro, E., *et al.*: Impact of model resolution on tropical cyclone simulation using the highresmp-primavera multimodel ensemble. *Journal of Climate* **33**(7), 2557–2583 (2020)
- [27] DeMaria, M., Franklin, J.L., Chirokova, G., Radford, J., DeMaria, R., Musgrave, K.D., Ebert-Uphoff, I.: Evaluation of tropical cyclone track and intensity forecasts from artificial intelligence weather prediction (aiwp) models. *arXiv preprint arXiv:2409.06735* (2024)
- [28] Dulac, W., Cattiaux, J., Chauvin, F., Bourdin, S., Fromang, S.: Assessing the representation of tropical cyclones in era5 with the cnrm tracker. *Climate Dynamics* **62**(1), 223–238 (2024)
- [29] Bloemendaal, N., Muis, S., Haarsma, R.J., Verlaan, M., Irazoqui Apecechea, M., de Moel, H., Ward, P.J., Aerts, J.C.: Global modeling

- of tropical cyclone storm surges using high-resolution forecasts. *Climate Dynamics* **52**(7), 5031–5044 (2019)
- [30] Lin, I., Chan, J.C.: Recent decrease in typhoon destructive potential and global warming implications. *Nature communications* **6**(1), 7182 (2015)
- [31] Tu, S., Hu, Z., Liang, M., Zhou, W., Chan, J.C., Xu, J.: Decreasing trend in destructive potential of tropical cyclones in the south indian ocean since the mid-1990s. *Communications Earth & Environment* **5**(1), 543 (2024)
- [32] Balaguru, K., Chang, P., Saravanan, R., Leung, L.R., Xu, Z., Li, M., Hsieh, J.-S.: Ocean barrier layers’ effect on tropical cyclone intensification. *Proceedings of the National Academy of Sciences* **109**(36), 14343–14347 (2012)
- [33] Manganello, J.V., Hodges, K.I., Kinter III, J.L., Cash, B.A., Marx, L., Jung, T., Achuthavarier, D., Adams, J.M., Altshuler, E.L., Huang, B., *et al.*: Tropical cyclone climatology in a 10-km global atmospheric gcm: toward weather-resolving climate modeling. *Journal of Climate* **25**(11), 3867–3893 (2012)
- [34] Haghroosta, T., Ismail, W., Ghafarian, P., Barekati, S.: The efficiency of the weather research and forecasting (wrf) model for simulating typhoons. *Natural Hazards and Earth System Sciences* **14**(8), 2179–2187 (2014)
- [35] Moon, J., Park, J., Cha, D.-H.: Does increasing model resolution improve the real-time forecasts of western north pacific tropical cyclones? *Atmosphere* **12**(6), 776 (2021)
- [36] Knapp, K.R., Kruk, M.C., Levinson, D.H., Diamond, H.J., Neumann, C.J.: The international best track archive for climate stewardship (ibtracs) unifying tropical cyclone data. *Bulletin of the American Meteorological Society* **91**(3), 363–376 (2010)
- [37] Zhang, J.A., Atlas, R., Emmitt, G.D., Bucci, L., Ryan, K.: Airborne doppler wind lidar observations of the tropical cyclone boundary layer. *Remote Sensing* **10**(6), 825 (2018)
- [38] Reichstein, M., Camps-Valls, G., Stevens, B., Jung, M., Denzler, J., Carvalhais, N., Prabhat, F.: Deep learning and process understanding for data-driven earth system science. *Nature* **566**(7743), 195–204 (2019)
- [39] Subich, C., Husain, S.Z., Separovic, L., Yang, J.: Fixing the double penalty in data-driven weather forecasting through a modified spherical harmonic loss function. *arXiv preprint arXiv:2501.19374* (2025)
- [40] Sun, X., Zhong, X., Xu, X., Huang, Y., Li, H., Neelin, J.D., Chen, D.,

- Feng, J., Han, W., Wu, L., *et al.*: A data-to-forecast machine learning system for global weather. *Nature Communications* **16**(1), 6658 (2025)
- [41] Lean, H.W., Theeuwes, N.E., Baldauf, M., Barkmeijer, J., Bessardon, G., Blunn, L., Bojarova, J., Boutle, I.A., Clark, P.A., Demuzere, M., *et al.*: The hectometric modelling challenge: Gaps in the current state of the art and ways forward towards the implementation of 100-m scale weather and climate models. *Quarterly Journal of the Royal Meteorological Society* **150**(765), 4671–4708 (2024)
- [42] Lopez-Gomez, I., Wan, Z.Y., Zepeda-Núñez, L., Schneider, T., Anderson, J., Sha, F.: Dynamical-generative downscaling of climate model ensembles. *Proceedings of the National Academy of Sciences* **122**(17), 2420288122 (2025)
- [43] Chen, A., Yuan, C.: Deep learning-based spatial downscaling and its application for tropical cyclone detection in the western north pacific. *Frontiers in Earth Science* **12**, 1345714 (2024)
- [44] Vosper, E., Watson, P., Harris, L., McRae, A., Santos-Rodriguez, R., Aitchison, L., Mitchell, D.: Deep learning for downscaling tropical cyclone rainfall to hazard-relevant spatial scales. *Journal of Geophysical Research: Atmospheres* **128**(10), 2022–038163 (2023)
- [45] Jing, R., Gao, J., Cai, Y., Xi, D., Zhang, Y., Fu, Y., Emanuel, K., Diffenbaugh, N.S., Bendavid, E.: Tc-gen: Data-driven tropical cyclone downscaling using machine learning-based high-resolution weather model. *Journal of Advances in Modeling Earth Systems* **16**(10), 2023–004203 (2024)
- [46] Guo, S., Chen, L., Niu, Z., Sun, Z., Zhang, X., Zhao, Y., Zhong, X., Li, H.: Fuxi-tc: A generative framework integrating deep learning and physics-based models for improved tropical cyclone forecasts. *arXiv preprint arXiv:2508.16168* (2025)
- [47] Niu, Z., Huang, W., Huang, S., Qin, B., Yang, M., Sun, H., Huo, Z., Xiao, H.: Intelligent shanghai typhoon model (istm): A generative probabilistic emulator for typhoon hybrid modeling. *arXiv preprint arXiv:2508.16851* (2025)
- [48] Baño-Medina, J., Sengupta, A., Steinhoff, D., Mulrooney, P., Nipen, T., Santa-Cruz, M., Nie, Y., Delle Monache, L.: A regional high resolution ai weather model for the prediction of atmospheric rivers and extreme precipitation. *npj Climate and Atmospheric Science* **8**(1), 385 (2025)
- [49] Mardani, M., Brenowitz, N., Cohen, Y., Pathak, J., Chen, C.-Y., Liu,

- C.-C., Vahdat, A., Nabian, M.A., Ge, T., Subramaniam, A., *et al.*: Residual corrective diffusion modeling for km-scale atmospheric downscaling. *Communications Earth & Environment* **6**(1), 124 (2025)
- [50] Sun, Q., Olschewski, P., Wei, J., Tian, Z., Sun, L., Kunstmann, H., Laux, P.: Key ingredients in regional climate modelling for improving the representation of typhoon tracks and intensities. *Hydrology and Earth System Sciences* **28**(4), 761–780 (2024)
- [51] Chen, B.-F., Chen, B., Hsiao, C.-M., Teng, H.-F., Lee, C.-S., Kuo, H.-C.: Constructing deep learning datasets to reveal climate trends of tropical cyclone intensity and structure extremes. *Artificial Intelligence for the Earth Systems* **4**(3), 240064 (2025)
- [52] Sun, Y.Q., Hassanzadeh, P., Zand, M., Chattopadhyay, A., Weare, J., Abbot, D.S.: Can ai weather models predict out-of-distribution gray swan tropical cyclones? *Proceedings of the National Academy of Sciences* **122**(21), 2420914122 (2025)
- [53] Zhong, X., Chen, L., Liu, J., Lin, C., Qi, Y., Li, H.: Fuxi-extreme: Improving extreme rainfall and wind forecasts with diffusion model. *Science China Earth Sciences* **67**(12), 3696–3708 (2024)
- [54] Lockwood, J.W., Gori, A., Gentine, P.: A generative super-resolution model for enhancing tropical cyclone wind field intensity and resolution. *Journal of Geophysical Research: Machine Learning and Computation* **1**(4), 2024-000375 (2024)
- [55] Price, I., Sanchez-Gonzalez, A., Alet, F., Andersson, T.R., El-Kadi, A., Masters, D., Ewalds, T., Stott, J., Mohamed, S., Battaglia, P., *et al.*: Probabilistic weather forecasting with machine learning. *Nature* **637**(8044), 84–90 (2025)
- [56] Ho, J., Jain, A., Abbeel, P.: Denoising diffusion probabilistic models. *Advances in neural information processing systems* **33**, 6840–6851 (2020)
- [57] Xiao, Z., Kreis, K., Vahdat, A.: Tackling the generative learning trilemma with denoising diffusion gans. *arXiv preprint arXiv:2112.07804* (2021)
- [58] Tao, N., Xie, F., Pan, B., Wang, H., Huang, H., Qiu, Z., Gui, K., Luo, J., Chen, X.: Efficient generative ai boosts probabilistic forecasting of sudden stratospheric warmings. *arXiv preprint arXiv:2510.26376* (2025)
- [59] Kornilov, N., Mokrov, P., Gasnikov, A., Korotin, A.: Optimal flow matching: Learning straight trajectories in just one step. *Advances in Neural Information Processing Systems* **37**, 104180–104204 (2024)

- [60] Lipman, Y., Chen, R.T., Ben-Hamu, H., Nickel, M., Le, M.: Flow matching for generative modeling. arXiv preprint arXiv:2210.02747 (2022)
- [61] Esser, P., Kulal, S., Blattmann, A., Entezari, R., Müller, J., Saini, H., Levi, Y., Lorenz, D., Sauer, A., Boesel, F., *et al.*: Scaling rectified flow transformers for high-resolution image synthesis. In: Forty-first International Conference on Machine Learning (2024)
- [62] Fotiadis, S., Brenowitz, N.D., Geffner, T., Cohen, Y., Pritchard, M., Vahdat, A., Mardani, M.: Adaptive flow matching for resolving small-scale physics. In: Forty-second International Conference on Machine Learning
- [63] Pérez-Alarcón, A., Vázquez, M., Trigo, R.M., Nieto, R., Gimeno, L.: Evaluation of wrf model configurations for dynamic downscaling of tropical cyclones activity over the north atlantic basin for lagrangian moisture tracking analysis in future climate. *Atmospheric Research* **307**, 107498 (2024)
- [64] Skamarock, W.C., Klemp, J.B., Dudhia, J., Gill, D.O., Liu, Z., Berner, J., Wang, W., Powers, J.G., Duda, M.G., Barker, D.M., *et al.*: A description of the advanced research wrf version 4. NCAR tech. note ncar/tn-556+str **145**(10.5065) (2019)
- [65] Hersbach, H., Bell, B., Berrisford, P., Hirahara, S., Horányi, A., Muñoz-Sabater, J., Nicolas, J., Peubey, C., Radu, R., Schepers, D., *et al.*: The era5 global reanalysis. *Quarterly journal of the royal meteorological society* **146**(730), 1999–2049 (2020)